

A Higgs Impostor in Low-Scale Technicolor

Estia Eichten^{1*}, Kenneth Lane^{2†} and Adam Martin^{3,4‡}

¹Theoretical Physics Group, Fermi National Accelerator Laboratory
P.O. Box 500, Batavia, Illinois 60510

²Department of Physics, Boston University
590 Commonwealth Avenue, Boston, Massachusetts 02215

³PH-TH Department, CERN
CH-1211 Geneva 23, Switzerland

⁴Department of Physics, University of Notre Dame[§]
Notre Dame, Indiana 46556

October 22, 2012

Abstract

We propose a “Higgs impostor” model for the 125 GeV boson, X , recently discovered at the LHC. It is a technipion, η_T , with $I^G J^{PC} = 0^- 0^{-+}$ expected in this mass region in low-scale technicolor. Its coupling to pairs of standard-model gauge bosons are dimension-five operators whose strengths are determined within the model. It is easy for $\sigma B(gg \rightarrow \eta_T \rightarrow \gamma\gamma)$ to agree with the observed two-photon rate, but $\eta_T \rightarrow ZZ^*, WW^* \rightarrow 4\text{leptons}$ are greatly suppressed relative to the standard-model Higgs rates. We therefore predict that the present $X \rightarrow ZZ^*, WW^*$ signals will be understood as backgrounds when more data is analyzed. This is a crucial and immediate test of our proposal. In our model the η_T mixes almost completely with the isovector π_T^0 , giving two similar states, η_L at 125 GeV and η_H higher, possibly in the range 170–190 GeV. Other important consequences of this mixing are (1) the only associated production of η_L is via $\rho_T \rightarrow W\eta_L$, and this could be sizable; (2) η_H may soon be accessible in $gg \rightarrow \eta_H \rightarrow \gamma\gamma$; and (3) LSTC phenomenology at the LHC is substantially modified.

*eichten@fnal.gov

†lane@physics.bu.edu

‡adam.martin@cern.ch

§Visiting scholar

1. Introduction

The stunning discovery by ATLAS and CMS of a new boson X at 125 GeV decaying into $\gamma\gamma$ and, at lower significance, ZZ^* and WW^* [1, 2] is widely suspected to be the long-sought Higgs boson of the standard model (SM) of electroweak interactions [3, 4, 5, 6, 7, 8]. As emphasized by Wilson (quoted in Ref. [9]) and ‘t Hooft [10], however, this resolution to the origin of electroweak symmetry breaking is very unsatisfactory. It is beset by the great problems of naturalness, hierarchy and flavor—the number, masses and mixings of the fermion generations. Notwithstanding this, the discovery clearly puts great pressure on technicolor, the scenario for the Higgs mechanism which needs no Higgs-like boson [11, 9]. This is especially true in low-scale technicolor (LSTC) [12, 13]. As far as we understand, there is no LSTC bound state that mimics H -decays in all these channels and at the rates expected on the basis of the observed $\sigma(pp \rightarrow X)B(X \rightarrow \gamma\gamma)$.^{1,2}

In this paper we propose that $X(125)$ is a state expected in a two-scale model of LSTC and which may be consistent with the data made public so far. This state is a would-be axion, a mixture of neutral isoscalar pseudoscalars occurring in each scale-sector that would be nearly massless if it were not for extended technicolor (ETC) interactions connecting the technifermions of the two scales. We call this particle the η_T . It has $CP = -1$.³ As we will see, $\sigma B(pp \rightarrow \eta_T \rightarrow \gamma\gamma)$ is probably larger than the corresponding SM Higgs cross section, and can easily match the current experimental observation. In the model we study, there is an unanticipated and interesting possibility: the η_T mixes, probably very substantially, with the neutral isovector π_T^0 expected in LSTC. This results in two states, η_L at 125 GeV and a heavier state η_H which, we will argue, is likely to be at 170–190 GeV. They have similar production and decay modes that are characteristic of both η_T and π_T^0 . We shall refer to our Higgs impostor as η_T in the absence of substantial mixing, or as η_L if mixing is important.

First, however, we ask: is $X(125)$ a Higgs boson? If over the next year or so the tentativeness of $X \rightarrow ZZ^*$ and WW^* is lifted and found to be in accord with the standard model and, say, $X \rightarrow \tau^+\tau^-$ and/or $\bar{b}b$ are seen, it will be irresistible to conclude that X is a Higgs boson, possibly the SM Higgs boson, H . At this early stage of X -physics studies, however, there are several discrepancies with the standard model or between the experiments that allow for an alternative explanation [1, 2, 27]:

¹There is a low-lying $I^G J^{PC} = 0^+ 0^{++}$ state in LSTC with many of the same decays as the standard model H , but its production rate is far too small to be the boson observed at the LHC [14]

²It is argued by some that walking technicolor or similar models have a light scalar due to their near-conformal invariance being spontaneously broken. This is called the “techni-dilaton”. It is also argued that it has Higgs-like couplings to gauge bosons and fermions; see e.g., Refs. [15, 16, 17, 18, 19, 20]. In our view, the existence of such a state is questionable. An interesting paper that discusses the phenomenology of a light dilaton while merely assuming its existence is Ref. [21].

³In addition to the dilaton papers cited above, others that have recently suggested a pseudoscalar Higgs impostor in the context of strong electroweak symmetry breaking include Refs. [22, 23, 24, 25, 26]. Unlike our model, most of these do not determine the energy scale and other factors in the dimension-five operators that couple the pseudoscalar to a pair of SM gauge bosons; see Eqs. (30)–(40).

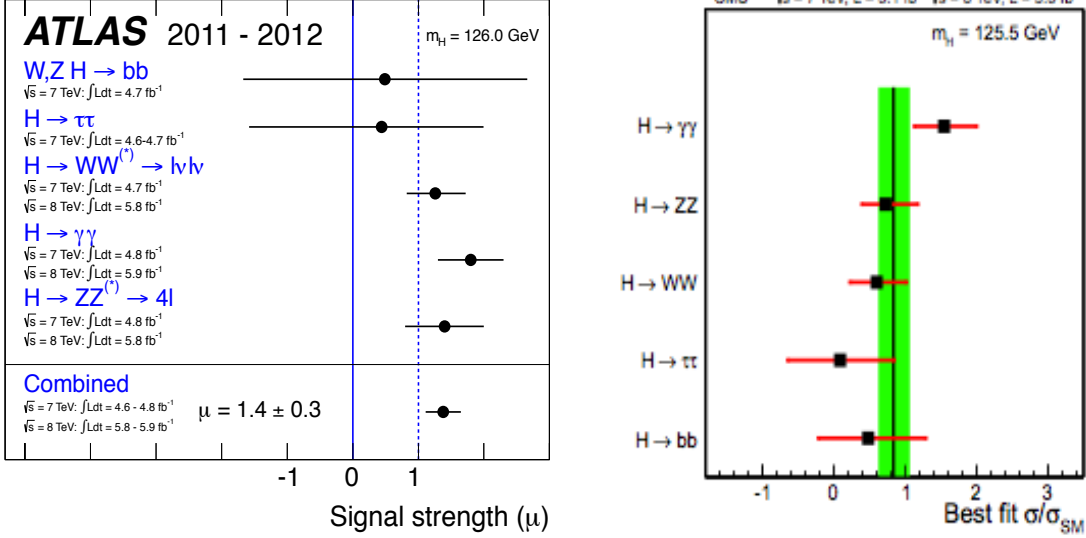


Figure 1: Comparisons of measured $X \rightarrow F$ production rates at the LHC with those for the standard-model Higgs boson, $\sigma B(pp \rightarrow X \rightarrow F)/\sigma B(pp \rightarrow H \rightarrow F)$, from ATLAS [1](left) and CMS [2].

1. Both ATLAS and CMS obtained $\sigma B(pp \rightarrow X \rightarrow \gamma\gamma) = 1.5\text{--}2.0$ times the rate $\sigma B(pp \rightarrow H \rightarrow \gamma\gamma)$ for the SM Higgs. These and other measured rates, compared to SM expectations, are summarized in Fig. 1.
2. Despite its low rate, the $X \rightarrow ZZ^* \rightarrow 4\ell$ channel is very important because of its excellent mass resolution. However, the CMS data at $M_{4\ell} \simeq 125 \text{ GeV}$ seems inconsistent with a particle of this mass decaying to ZZ^* . In Fig. 2 only two of the ten points in the M_{Z1} vs. M_{Z2} plot for the 4-lepton data at this mass appear to have a real Z -boson in them, much less than expected at 125 GeV, as the CMS Monte Carlo in the figure shows. The corresponding 2-D plot for ATLAS, also in Fig. 2 looks more like what would be expected for a Higgs, with 6–8 of 13 events in the signal region. This difference may just be statistical. However, the ATLAS real ZZ data is systematically higher than its calculated background while the CMS ZZ data and expected background are in reasonably good agreement; see Fig. 3. We do not know if this impacts the $M_{4\ell} < 2M_Z$ region.
3. The $X \rightarrow WW^* \rightarrow \ell\nu\ell\nu$ channel is also important, but not nearly so much as $ZZ^* \rightarrow 4\ell$ because of the large missing energy and lack of a clearly discrete mass for its source. Furthermore, the ATLAS and CMS data for $X \rightarrow WW^* \rightarrow \ell\nu\ell\nu$ also appear somewhat inconsistent. ATLAS's combined 7 and 8-TeV data gives $\sigma B(pp \rightarrow X \rightarrow WW^*) = (1.4 \pm 0.5) \times \sigma B(pp \rightarrow H \rightarrow WW^*)$ at $M_X \sim 125 \text{ GeV}$ while CMS obtained $\simeq 0.6 \pm 0.4 \times \sigma B(pp \rightarrow H \rightarrow WW^*)$; see Fig. 1. As for $ZZ^* \rightarrow 4\ell$, the ATLAS 8-TeV data

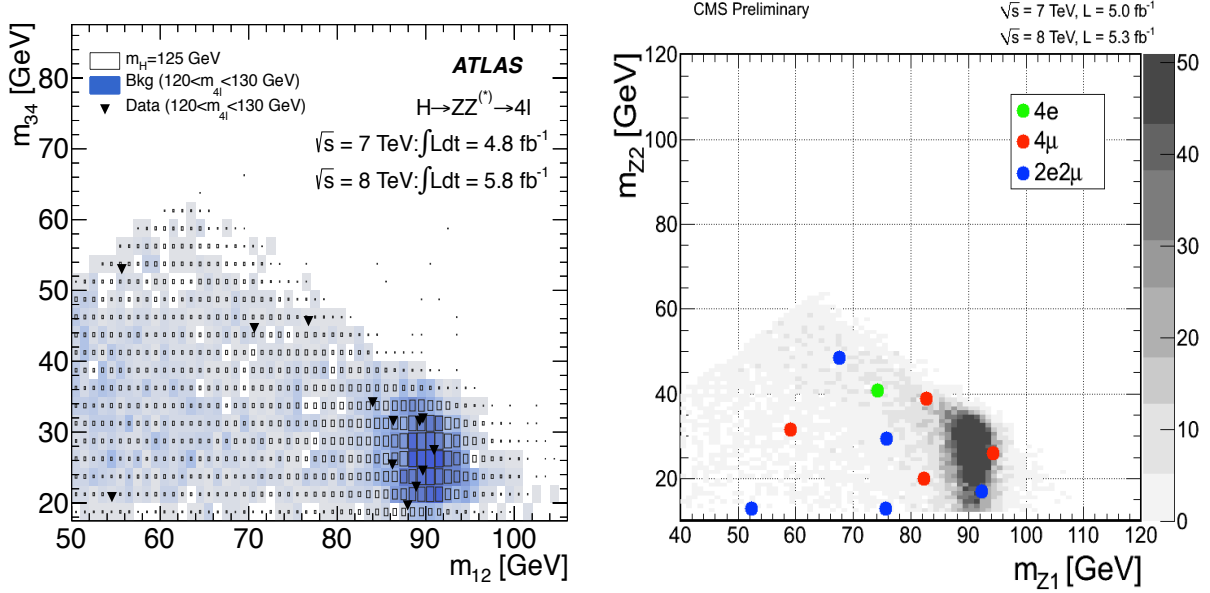


Figure 2: The Dalitz plot of high vs. low dilepton mass in the region $M_{4\ell} \simeq 125$ GeV from ATLAS [1] (left) and CMS [27] (right). See the text for comments.

appears to be generally higher than the SM Higgs expectation.

4. The CMS search for $X \rightarrow \tau^+ \tau^-$ found no significant departure from the standard model background and set a limit of $\sigma B(pp \rightarrow X \rightarrow \tau^+ \tau^-) = 1.06 \times \sigma B(pp \rightarrow H \rightarrow \tau^+ \tau^-)$ at 125 GeV. At this writing, ATLAS has released nothing on its search for $X \rightarrow \tau^+ \tau^-$.
5. Neither ATLAS nor CMS has found the associated production mode $WX \rightarrow \ell \nu \bar{b} b$, but this is not surprising given the large backgrounds to this signal at the LHC. The CDF and DØ experiments have combined their search for $\bar{p}p \rightarrow WH, ZH$ with $H \rightarrow \bar{b} b$ and claimed a signal consistent with $X(125)$ at the 3.1σ level [28]. This is surprising considering since $S/B < 1\%$ for the samples used for this channel [29]. Moreover, as Fig. 4 shows, the broad mass peak and its significance are strongest at $M_{\bar{b}b} = 135$ GeV. Finally, the CDF-DØ paper does not make clear what correction was made for lost neutrinos and muons in the 40% of b -semileptonic decays in $\bar{b}b$ states. Therefore, the actual $\bar{b}b$ mass peak might be even higher, closer to 145–150 GeV [30].

Of course, all of these disagreements may disappear with more data. For now, they are tantalizing, and alternative interpretations of $X(125)$ are worth exploring.

In Sec. 2 we present a two-scale model for the η_T . This model is not unique, but it is simple. Because the η_T is a pseudo-Goldstone boson with $CP = -1$, all its interactions with a pair of SM gauge bosons are of the nonrenormalizable Wess-Zumino-Witten (WZW) type [31, 32]. Compared to the SM Higgs boson, this implies very little $\eta_T \rightarrow WW^*, ZZ^*$, associated production of η_T with W or Z , and vector boson fusion (VBF) of η_T via WW

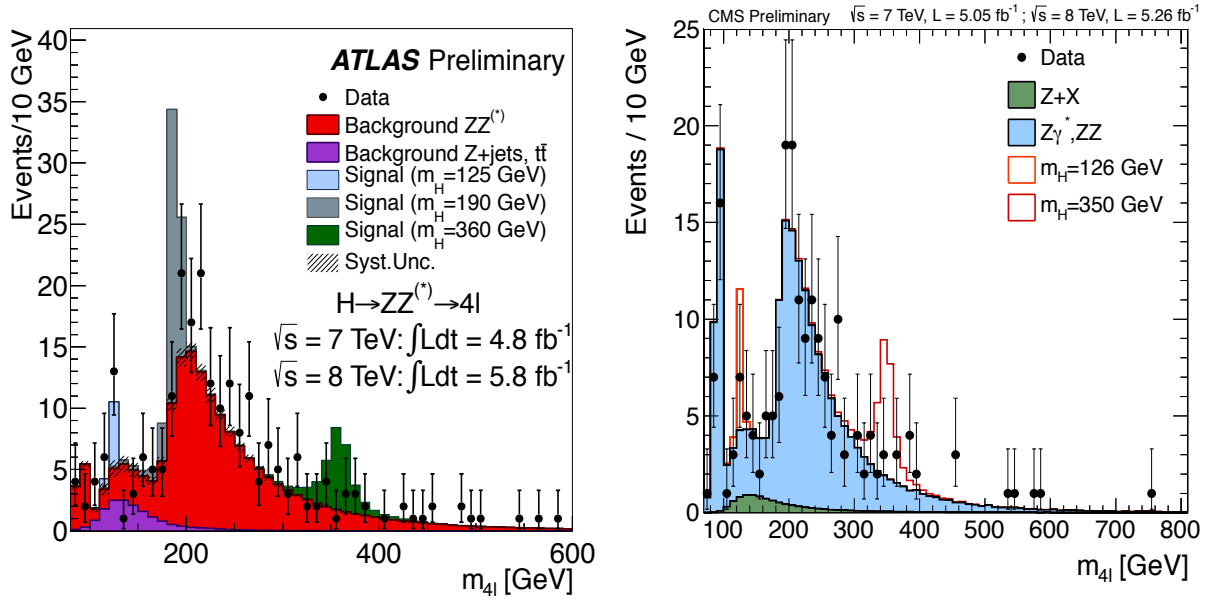


Figure 3: Four-lepton invariant mass distributions in the ZZ^* and on-shell ZZ mass regions from ATLAS [1] (left) and CMS [27] (right). See the text for comments.

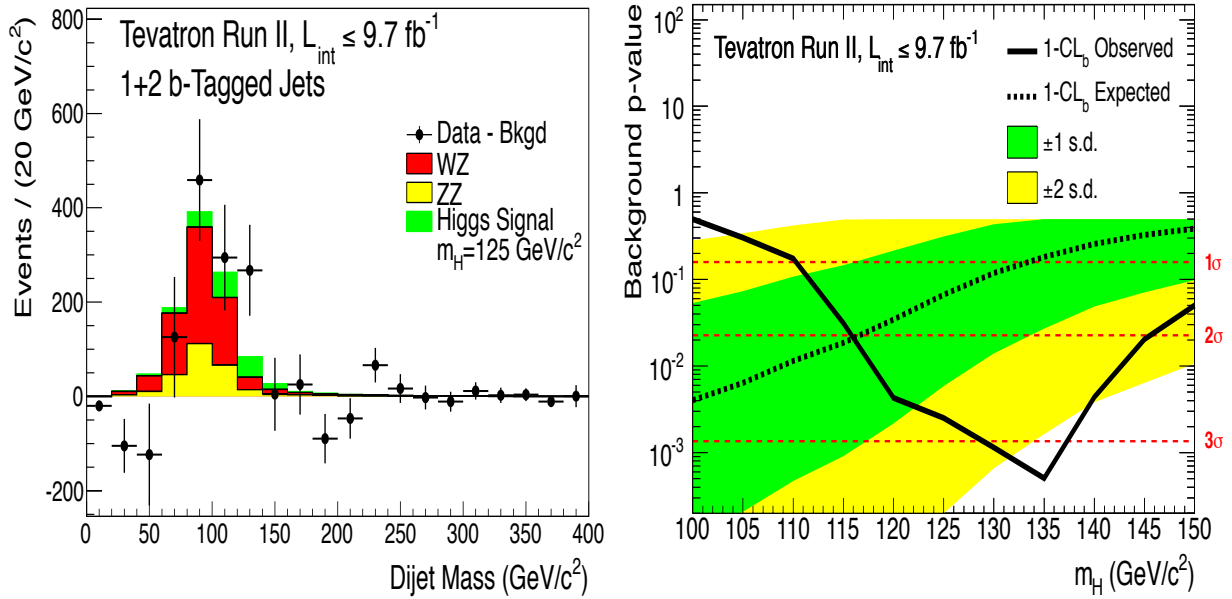


Figure 4: CDF and DØ data on $\bar{p}p \rightarrow W\bar{b}b$ with $M_{\bar{b}b}$ in the 125 GeV region [28]. See the text for comments.

and ZZ . In Sec. 3 we discuss mixing of the isoscalar η_T with the isovector π_T^0 . This mixing is essentially complete in our model and we believe this is a general feature of two-scale models with rather widely separated energy scales. This gives two states, η_L at 125 GeV

and a similar state η_H at higher mass. If the dijet excess reported by CDF [30] is real and is described by LSTC [33] then $M_{\eta_H} = 170\text{--}190\text{ GeV}$. We urge a search for such a state decaying to two photons. Furthermore, this mixing opens up the possibility of associated production of η_L with W , but not Z , via the resonant process $\rho_T^\pm \rightarrow W^\pm \eta_L$. Since η_L decays nearly 100% of the time to gg , this will pollute the SM $WW/WZ \rightarrow \ell\nu jj$ signal *and* the CDF dijet excess.

The WZW interactions of our Higgs impostor are determined in Sec. 4 for the unmixed and mixed cases. We also discuss there its couplings to fermion pairs; these are induced by ETC and are, therefore, rather uncertain. The phenomenology of η_L is presented in Sec. 5. In detail, it is specific to our two-scale model, but the general features, especially those dictated by the WZW interactions, will hold in any such model. In particular: (1) By far, the dominant η_L -production mechanism is via gluon fusion. Associated production with W depends on the mixing of η_T with π_T^0 . There is very little associated production with Z , and very little VBF via WW and ZZ . Generally, we find that $\sigma(gg \rightarrow \eta_L) \gg \sigma(gg \rightarrow H)$. Obtaining the correct $\sigma B(gg \rightarrow \eta_L \rightarrow \gamma\gamma)$ rate is then due to a fortuitous (but ubiquitous) cancellation among the terms in the $\gamma\gamma$ amplitude. (2) The branching ratios $B(\eta_L \rightarrow ZZ^*, WW^* \rightarrow \text{leptons})$ are extremely small. Therefore, according to our model's general framework, what has been observed by CMS and ATLAS must be background. (3) The branching ratios of η_L to $\tau^+\tau^-$ and $b\bar{b}$ may be sizable or not, depending on the unknown couplings in the underlying ETC model. In Sec. 6 we summarize the consequences of η_T - π_T^0 mixing on the low-scale ρ_T phenomenology at the LHC. These are dramatic if the mixing is as large as we find in Sec. 3, generally making it more difficult to detect the signatures we discussed in Ref. [34].

2. A Two-Scale Model for the η_T

The technipion η_T is a pseudo-Goldstone boson that must occur in LSTC models [12]. It was referred to as π_T^0 in previous papers, e.g., Ref. [13], which also contains a more complete description of LSTC. Since η_T decays to two photons, it has $CP = -1$ and, so, it has no renormalizable couplings to a pair of SM gauge bosons. Its main production mechanism, therefore, must be via gluon (gg) fusion. This requires that η_T be composed, at least in part, of technifermions carrying ordinary $SU(3)_C$ color.⁴ In LSTC, we usually assume that the lightest (lowest-scale) technifermions are $SU(3)_C$ -singlets, and we make that assumption here. Thus, for an $\eta_T gg$ interaction to occur, the higher-scale technifermions must be

⁴The top quark cannot couple strongly to η_T nor any other π_T because, in ETC models with fermion-bilinear anomalous dimension $\gamma_m \leq 1$ [35], m_t must arise from some other strong interaction, such as topcolor [36].

colored.⁵ To describe this, we adopt the following two-scale model:

$$\begin{aligned} \text{Scale 1: } T_1 &\equiv \begin{pmatrix} U_1 \\ D_1 \end{pmatrix} = \begin{cases} T_{1L} &= (\square, 1, 2)_{Y_1} \\ U_{1R} &= (\square, 1, 1)_{Q_{U1}} \\ D_{1R} &= (\square, 1, 1)_{Q_{D1}} \end{cases} \\ \text{Scale 2: } T_2 &\equiv \begin{pmatrix} U_2 \\ D_2 \end{pmatrix} = \begin{cases} T_{2L} &= (\square, \square, 2)_{Y_2} \\ U_{2R} &= (\square, \square, 1)_{Q_{U2}} \\ D_{2R} &= (\square, \square, 1)_{Q_{D2}} \end{cases} \end{aligned} \quad (1)$$

under $(SU(N_{TC}), SU(3)_C, SU(2))_{U(1)}$.

We emphasize that this model's purpose is to illustrate our LSTC proposal to account for the $X(125)$ data. Different TC representations and/or input parameters (N_{TC} , etc.) could give quantitatively different results, and more data may require a refinement of the model. Nevertheless, we believe the model's general features—the interactions η_T has with ordinary matter and the typical strength of these interactions—will survive as long as the idea of an LSTC impostor of $X(125)$ does.

When the technifermions T_1 and T_2 condense, there are a number of Goldstone bosons (all but three of which must get mass from ETC interactions [38]) including two color-singlets with $I^G J^{PC} = 0^+ 0^{-+}$ we call η_1 and η_2 . These couple to the $U(1)$ axial vector currents $j_{i,5\mu} = \frac{1}{2} \bar{T}_i \gamma_\mu \gamma_5 T_i$ as

$$\langle \Omega | j_{1,5\mu} | \eta_1(p) \rangle = i F_1 p_\mu, \quad \langle \Omega | j_{2,5\mu} | \eta_2(p) \rangle = i \sqrt{3} F_2 p_\mu, \quad (2)$$

where F_1 and F_2 are the basic (canonically normalized) π_T decay constants of scales 1 and 2. They are related to the weak decay constant $F_\pi \equiv v = 246 \text{ GeV}$ and the LSTC mixing angle parameter $\sin \chi$ [39, 13] by

$$F_\pi = \sqrt{F_1^2 + 3F_2^2}, \quad F_1 = F_\pi \sin \chi, \quad \sqrt{3} F_2 = F_\pi \cos \chi. \quad (3)$$

A recent search by CMS for $\rho_T \rightarrow WZ \rightarrow 3\ell\nu$ put a 95% upper limit of about 20 fb on its cross section at $M_{\rho_T} = 275\text{--}290 \text{ GeV}$ and $M_{\pi_T} > 140 \text{ GeV}$ [37]. This requires $\sin \chi \lesssim 0.30$ for the LSTC model with these masses [34]. While this bound is relevant for the case of little or no η_T - π_T^0 mixing, sizable mixing weakens it; see Sec. 6.

The $U(1)$ currents have divergences with TC-gluon anomalous terms and other explicit breaking:

$$\partial^\mu j_{i,5\mu} = -\frac{g_{TC}^2}{16\pi^2} N_i G_{T,\mu\nu} \tilde{G}_T^{\mu\nu} + i[\mathcal{Q}_{i,5}, \mathcal{H}_{ETC}] + \dots, \quad (4)$$

where $\mathcal{Q}_{i,5} = \int d^3x j_{i,50}$, \mathcal{H}_{ETC} is a 4-technifermion interaction involving T_1 and T_2 , and the ellipses are $SU(3)_C \otimes SU(2) \otimes U(1)$ anomalous divergences that will be specified in Sec. 4. In

⁵An alternative in which the lightest-scale technifermions are colored might be interesting, but we shall not consider it here. As Eq. (3) indicates, this tends to imply a larger value of the LSTC parameter $\sin \chi$ in Eq. (3) and that is disfavored experimentally [37, 34].

Eq.(4) the numerical factors are $N_i = 2T(R_{TC,i})d(R_{C,i})$, where the factor 2 is for isodoublet technifermions, $T(R_{TC})$ is the trace of a square of generators for TC-representation R ($= \frac{1}{2}$ for fundamentals of SUN)) and $d(R_C)$ is the dimension of the $SU(3)_C$ representation. In the model of Eq. (1),

$$N_1 = 2 \cdot \frac{1}{2} \cdot 1 = 1, \quad , N_2 = 2 \cdot \frac{1}{2}(N_{TC} - 2) \cdot 3 = 3(N_{TC} - 2). \quad (5)$$

The current $j'_{5\mu} = j_{1,5\mu} + j_{2,5\mu}$ is conserved by ETC interactions (see Sec. 3) but not by the TC anomaly:

$$\partial^\mu j'_{5\mu} = -\frac{g_{TC}^2}{16\pi^2}(N_1 + N_2)G_{T,\mu\nu}\tilde{G}_T^{\mu\nu} + \dots. \quad (6)$$

It couples to a linear combination η'_T of η_1 and η_2 which gets its mass mainly from TC instantons and is heavy. The orthogonal linear combination is the η_T and its mass arises from \mathcal{H}_{ETC} . It couples to the TC-anomaly-free current

$$j_{5\mu} = N_2 j_{1,5\mu} - N_1 j_{2,5\mu} \quad (7)$$

$$\partial^\mu j_{5\mu} = i[N_2 \mathcal{Q}_{1,5} - N_1 \mathcal{Q}_{2,5}, \mathcal{H}_{ETC}] + \dots = i(N_1 + N_2)[\mathcal{Q}_{1,5}, \mathcal{H}_{ETC}] + \dots. \quad (8)$$

Let us write

$$\begin{aligned} |\eta'_T\rangle &= |\eta_1\rangle \sin \eta + |\eta_2\rangle \cos \eta \\ |\eta_T\rangle &= |\eta_1\rangle \cos \eta - |\eta_2\rangle \sin \eta. \end{aligned} \quad (9)$$

The mixing angle η is determined by noting that, if $\langle \Omega | j_{5\mu} | \eta'_T \rangle \neq 0$ in the limit $\mathcal{H}_{ETC} \rightarrow 0$, then $M_{\eta'_T} \cong 0$ since the current is TC-anomaly free. This yields

$$\sin \eta = \frac{\sqrt{3}N_1 F_2}{F_{\eta_T}}, \quad \cos \eta = \frac{N_2 F_1}{F_{\eta_T}}, \quad \text{where} \quad F_{\eta_T} = \sqrt{N_2^2 F_1^2 + 3N_1^2 F_2^2}. \quad (10)$$

Noting that

$$F_{\eta_T} = \sqrt{N_2^2 \sin^2 \chi + N_1^2 \cos^2 \chi} F_\pi, \quad (11)$$

we have

$$\sin \eta = \frac{N_1 \cos \chi}{\sqrt{N_2^2 \sin^2 \chi + N_1^2 \cos^2 \chi}}, \quad \cos \eta = \frac{N_2 \sin \chi}{\sqrt{N_2^2 \sin^2 \chi + N_1^2 \cos^2 \chi}}. \quad (12)$$

For $N_{TC} = 4$ and $\sin \chi = 0.3$, we have $N_1 = 1$, $N_2 = 6$, $\sin \eta = 0.468$, $\cos \eta = 0.884$, and $F_{\eta_T} = 501 \text{ GeV}$ is the normalized decay constant of the η_T .

3. η_T - π_T^0 Mixing

The state η_T discussed in Sec. 2 generally is not a mass eigenstate. In the model we have presented and in similar ones, the ETC interactions that give it mass also mix it with

the neutral isovector technipion π_T^0 discussed in Refs. [33, 34]. This effects not only η_T phenomenology but, as we discuss in Sec. 6, the LSTC description of the CDF dijet excess observed near $M_{jj} = 150$ GeV in Wjj production [30, 40]. The ETC interactions of T_1 and T_2 must be $SU(N_{TC}) \otimes SU(3)_C \otimes SU(2) \otimes U(1)$ invariant. For our model they have the following form at energies far below the masses $M_{1,2,3}$ of ETC gauge bosons:

$$\begin{aligned}\mathcal{H}_{ETC} &= \frac{g_{ETC}^2}{M_1^2} \bar{T}_{1L} \gamma^\mu T_{1L} \bar{T}_{1R} \gamma_\mu (a_1 + b_1 \tau_3) T_{1R} \\ &+ \frac{g_{ETC}^2}{M_2^2} (\bar{T}_{1L} \gamma^\mu T_{2L} \bar{T}_{2R} \gamma_\mu (a_2 + b_2 \tau_3) T_{1R} + \text{h.c.}) \\ &+ \frac{g_{ETC}^2}{M_3^2} \bar{T}_{2L} \gamma^\mu T_{2L} \bar{T}_{2R} \gamma_\mu (a_3 + b_2 \tau_3) T_{2R}.\end{aligned}\quad (13)$$

The $SU(N_{TC}) \otimes SU(3)_C$ indices of these interactions are suppressed, but the structure of the middle term, e.g., is

$$\bar{T}_{1L}^\alpha \gamma^\mu T_{2L}^{[\alpha\beta],k} \bar{T}_{2R}^{[\alpha\gamma],k} \gamma_\mu (a_2 + b_2 \tau_3) T_{1R}^\gamma, \quad (14)$$

where $\alpha, \beta, \gamma = 1, 2, \dots, N_{TC}$ are $SU(N_{TC})$ indices with $[\alpha\beta] = -[\beta\alpha]$ and $k = 1, 2, 3$ is an $SU(3)_C$ index. The $SU(2)_R$ violation in the b -terms is necessary to split up from down-fermions. We expect $a_i, |b_i| = \mathcal{O}(1)$ with $a_i > 0$ while b_i may have either sign.

The masses and mixing of the technipions π_T^\pm, π_T^0 and η_T come entirely from the $\bar{T}_1 T_2 \bar{T}_2 T_1$ terms, and they are determined as follows: In the absence of η_T - π_T^0 mixing, the mass eigenstates $|\pi_T^a\rangle$ ($a = 1, 2, 3$) are the linear combination

$$|\pi_T^a\rangle = \cos \chi |\pi_1^a\rangle - \sin \chi |\pi_2^a\rangle, \quad (15)$$

where $|\pi_{1,2}^a\rangle$ are the scale-1,2 technipions. The mixing angle χ was defined in Eq. (3), with $\sin \chi > 0$. The orthogonal combinations are the three Goldstone components of the electroweak bosons, $|W_L^a\rangle$. The state $|\pi_T^a\rangle$ does not couple to the conserved electroweak axial current $j_{5\mu}^{a,EW} = j_{1,5\mu}^a + j_{2,5\mu}^a + \dots$, where $j_{i,5\mu}^a = \frac{1}{2} \bar{T}_i \gamma_\mu \gamma_5 \tau_a T_i$; if it did, $M_{\pi_T} = 0$. The π_T^a current we will use for calculating M_{π_T} is

$$j_{5\mu}^a = j_{1,5\mu}^a \cot \chi - j_{2,5\mu}^a \tan \chi. \quad (16)$$

This current couples to π_T in Eq. (15) with strength F_π ,

$$\langle \Omega | j_{5\mu}^a | \pi_T^b(p) \rangle = i F_\pi p_\mu \delta_{ab}, \quad (17)$$

but not to the orthogonal combination, the erstwhile Goldstone bosons that are the longitudinally-polarized W^\pm and Z . Then, with $\mathcal{Q}_5^a = \int d^3x j_{50}^a$ for $a = 1, 2, 3$, and using isospin and parity invariance of the vacuum state $|\Omega\rangle$, we obtain [41]

$$\begin{aligned}F_\pi^2 M_{\pi_T}^2 &= i^2 \langle \Omega | [\mathcal{Q}_5^a, [\mathcal{Q}_5^a, \mathcal{H}_{ETC}]] | \Omega \rangle \\ &= \frac{i^2 a_2 g_{ETC}^2}{2 M_2^2 \sin^2 \chi \cos^2 \chi} \langle \Omega | [\bar{T}_{1L} \gamma^\mu \tau_a T_{2L} \bar{T}_{2R} \gamma_\mu \tau_a T_{1R} + \bar{T}_{1L} \gamma^\mu T_{2L} \bar{T}_{2R} \gamma_\mu T_{1R} + \text{h.c.}] | \Omega \rangle \\ &= \frac{2 i^2 a_2 g_{ETC}^2}{M_2^2 \sin^2 \chi \cos^2 \chi} \langle \Omega | [\bar{T}_{1L} \gamma^\mu T_{2L} \bar{T}_{2R} \gamma_\mu T_{1R}] | \Omega \rangle,\end{aligned}\quad (18)$$

Similarly, with $\mathcal{Q}_5 = N_2 \mathcal{Q}_{1,5} - N_1 \mathcal{Q}_{2,5}$, we get

$$F_{\eta_T}^2 M_{\eta_T}^2 = [(N_1 + N_2) \sin \chi \cos \chi F_\pi M_{\pi_T}]^2 \quad (19)$$

$$F_\pi F_{\eta_T} M_{\eta_T \pi_T^0}^2 = (b_2/a_2)(N_1 + N_2) \sin \chi \cos \chi F_\pi^2 M_{\pi_T}^2. \quad (20)$$

$$(21)$$

Then, using Eq. (11) for F_{η_T} ,

$$\left(\frac{M_{\eta_T}}{M_{\pi_T}}\right)^2 = \frac{((N_1 + N_2) \sin \chi \cos \chi)^2}{N_1^2 + (N_2^2 - N_1^2) \sin^2 \chi} = 0.967 (0.998), \quad (22)$$

$$\left(\frac{M_{\eta_T \pi_T^0}}{M_{\pi_T}}\right)^2 = \frac{b_2}{a_2} \left(\frac{M_{\eta_T}}{M_{\pi_T}}\right)^2. \quad (23)$$

Here, M_{π_T} is the mass of the charged π_T^\pm , which is unaffected by the $|\Delta I| = 1$ isospin breaking in \mathcal{H}_{ETC} . The numerical values in Eq. (22) are for $\sin \chi = 0.30$ and $N_{TC} = 4(6)$. They will be close to one when $(N_2 \sin \chi)^2 \gg N_1^2$ and $\sin^2 \chi \ll 1$, as it is here.

Thus, in two-scale models like the one presented here, we have the surprising result that the mass eigenstates are nearly 50-50 admixtures of the neutral isoscalar and isovector technipions,

$$\begin{aligned} |\eta_L\rangle &\cong \sqrt{\frac{1}{2}} (|\eta_T\rangle - \text{sgn}(b_2) \pi_T^0), \\ |\eta_H\rangle &\cong \sqrt{\frac{1}{2}} (|\eta_T\rangle + \text{sgn}(b_2) \pi_T^0), \end{aligned} \quad (24)$$

with masses

$$M_{\eta_L} \cong M_{\pi_T} \sqrt{1 - |b_2|/a_2}, \quad M_{\eta_H} \cong M_{\pi_T} \sqrt{1 + |b_2|/a_2}. \quad (25)$$

How do we determine the mass of η_H ? One way is this: In recent work [33, 34] we ascribed the CDF dijet mass excess near 150 GeV [30, 40] to the production and decay of the lightest isovector technipions, produced in the LSTC process $\rho_T \rightarrow W \pi_T \rightarrow \ell \nu jj$. In the present framework, we assume that what CDF saw was $\rho_T^0 \rightarrow W^\pm \pi_T^\mp$, with $M_{\pi_T^\pm} = 150\text{--}160$ GeV. The π_T^0 is now part of the mixed-state η_L , our Higgs impostor, observed by ATLAS and CMS with mass 125 GeV. Then, from Eq. (25), $M_{\eta_H} = 170\text{--}190$ GeV. In Sec. 6, we will see how this interpretation alters LSTC phenomenology at the LHC.⁶ This rather precise prediction for M_{η_H} is satisfying, but it does rely on our description of the CDF excess. If we gave up that description, we would still expect that the η_H —a pseudo-Goldstone boson composed mainly of lighter scale technifermions—would not be very much heavier than η_L . This is clear from Eqs. (25). The converse expectation is also true: If $X(125)$ is to be interpreted as an η_T of low-scale technicolor, then there must be other technihadron states nearby, and they should be accessible in hadron collider experiments.

⁶We now estimate the Tevatron rate for $W^\pm \pi_T^\mp$ production is about 2.4 pb, essentially unchanged from our prediction in Ref. [33]. This estimate is very rough because the PYTHIA code does not properly describe the model with η_T - π_T^0 mixing [42].

4. η_T and π_T^0 Interactions

The couplings between the CP -odd η_T and a pair of SM gauge bosons or SM fermion-antifermion pairs ($\bar{f}f$) are given by

$$\begin{aligned}\mathcal{L}_{\eta_T} &= \frac{\eta_T}{F_{\eta_T}} \partial^\mu j_{5\mu} \equiv \frac{\eta_T}{F_{\eta_T}} \partial^\mu (N_2 j_{1,5\mu} - N_1 j_{2,5\mu}) \\ &= \text{SM gauge boson anomaly terms} + i[\mathcal{Q}_5, \mathcal{H}_{ETC}].\end{aligned}\quad (26)$$

A similar expression holds for π_T^0 with $F_{\pi_T} \equiv F_\pi$.

The anomaly terms are contained in the gauged WZW interaction calculated in Refs [31, 32]. For interactions involving chiral gauge groups, the simplest way to calculate them is to expand the WZW term to linear order in the technipion fields. We can use the formalism of Refs. [31, 32] by introducing a nonlinear-sigma formulation of our setup, specifically,

$$\Sigma_1 = \exp\left(\frac{2i\boldsymbol{\pi}_1}{F_1}\right), \quad \Sigma_2 = \exp\left(\frac{2i\boldsymbol{\pi}_2}{\sqrt{3}F_2}\right), \quad (27)$$

with covariant derivative

$$\begin{aligned}D_\mu \Sigma_i &= \partial_\mu \Sigma_i - i\mathcal{A}_L \Sigma_i + i\Sigma_i \mathcal{A}_R, \\ \mathcal{A}_L &= \frac{1}{2} (gW_\mu^a \tau_a + g'Y_i B_\mu \tau_0), \\ \mathcal{A}_R &= \frac{1}{2} g' B_\mu (\tau_3 + Y_i \tau_0).\end{aligned}\quad (28)$$

Here, $\boldsymbol{\pi}_i = \frac{1}{2}(\pi_i^a \tau_a + \eta_i \tau_0)$, where $\tau_0 = \mathbf{1}_2$, and F_1, F_2 are the scale-1,2 technipion decay constants defined earlier. Applying this setup to Eq. (69) of Ref. [43], each techni-sector contributes a WZW term weighted by a coefficient that depends on the number of degrees of freedom in that sector. The total WZW interaction is then $\mathcal{L}_{WZW,tot} = \mathcal{L}_{WZW,1} + \mathcal{L}_{WZW,2}$,

For η_T, π_T interactions involving vectorial gauge groups, such as $\eta_T \rightarrow \gamma\gamma$ or $\eta_T \rightarrow gg$, the WZW result has the familiar form,

$$\partial^\mu j_{i,5\mu} = -\frac{g_A^2}{32\pi^2} \text{Tr}(\tau_0 \{t_{i,a}^A, t_{i,b}^A\}) G_{\mu\nu}^{Aa} \tilde{G}^{Ab,\mu\nu}, \quad (29)$$

where $t_{i,a}^A$ is the a -th generator of technifermion doublet T_i in gauge group A . The corresponding expression for $\partial^\mu j_{5\mu}^3$ has the trace $\text{Tr}(\tau_3 \{t_{i,a}^A, t_{i,b}^A\})$.

Since only the isoscalar η_2 couples strongly to $SU(3)_C$ gluons through a loop of the color-triplet T_2 -fermions (see footnote 3), we have

$$\mathcal{L}_{\eta_T gg} = \sqrt{2} \mathcal{L}_{\eta_L, H gg} = \frac{g_C^2}{64\pi^2 F_{\eta_T}} [N_1 N_{TC} (N_{TC} - 1)] \eta_T G_{C,\mu\nu}^\alpha \tilde{G}_C^{\alpha,\mu\nu}. \quad (30)$$

Because of the large numerator, this operator typically will be substantially stronger than the standard H coupling to two gluons.

The nonzero WZW couplings of η_T and π_T^0 to a pair of $SU(2) \otimes U(1)$ bosons are

$$\mathcal{L}_{\eta_T BB} = -\frac{g'^2 N_{TC}}{96\pi^2 F_{\eta_T}} \left[N_2(1 + 12Y_1^2) - \frac{3}{2}N_1(N_{TC} - 1)(1 + 12Y_2^2) \right] \eta_T B_{\mu\nu} \tilde{B}^{\mu\nu}, \quad (31)$$

$$\mathcal{L}_{\eta_T WW} = -\frac{g^2 N_{TC}}{96\pi^2 F_{\eta_T}} \left[N_2 - \frac{3}{2}N_1(N_{TC} - 1) \right] \eta_T W_{\mu\nu}^a \tilde{W}^{a,\mu\nu}, \quad (32)$$

$$\mathcal{L}_{\eta_T WB} = -\frac{gg' N_{TC}}{96\pi^2 F_{\eta_T}} \left[N_2 - \frac{3}{2}N_1(N_{TC} - 1) \right] \eta_T W_{\mu\nu}^3 \tilde{B}^{\mu\nu}, \quad (33)$$

$$\mathcal{L}_{\pi_T^0 BB} = -\frac{g'^2 N_{TC}}{16\pi^2 F_\pi} \left[Y_1 \cot \chi - \frac{3}{2}(N_{TC} - 1)Y_2 \tan \chi \right] \pi_T^0 B_{\mu\nu} \tilde{B}^{\mu\nu}, \quad (34)$$

$$\mathcal{L}_{\pi_T^0 WB} = -\frac{gg' N_{TC}}{16\pi^2 F_\pi} \left[Y_1 \cot \chi - \frac{3}{2}(N_{TC} - 1)Y_2 \tan \chi \right] \pi_T^0 W_{\mu\nu}^3 \tilde{B}^{\mu\nu}. \quad (35)$$

From these we obtain

$$\mathcal{L}_{\eta_T \gamma\gamma} = -\frac{e^2 N_{TC}}{32\pi^2 F_{\eta_T}} \left[N_2(1 + 4Y_1^2) - \frac{3}{2}N_1(N_{TC} - 1)(1 + 4Y_2^2) \right] \eta_T F_{\mu\nu} \tilde{F}^{\mu\nu}, \quad (36)$$

$$\begin{aligned} \mathcal{L}_{\eta_T Z\gamma} = & -\frac{e\sqrt{g^2 + g'^2} N_{TC}}{32\pi^2 F_{\eta_T}} \left[N_2(1 - 2(1 + 4Y_1^2)\sin^2 \theta_W) \right. \\ & \left. - \frac{3}{2}N_1(N_{TC} - 1)(1 - 2(1 + 4Y_2^2)\sin^2 \theta_W) \right] \eta_T F_{\mu\nu} \tilde{Z}^{\mu\nu}, \end{aligned} \quad (37)$$

$$\begin{aligned} \mathcal{L}_{\eta_T ZZ} = & -\frac{(g^2 + g'^2) N_{TC}}{96\pi^2 F_{\eta_T}} \left\{ N_2 \left[1 - 3\sin^2 \theta_W + 3(1 + 4Y_1^2)\sin^4 \theta_W \right] \right. \\ & \left. - \frac{3}{2}N_1(N_{TC} - 1) \left[1 - 3\sin^2 \theta_W + 3(1 + 4Y_2^2)\sin^4 \theta_W \right] \right\} \eta_T Z_{\mu\nu} \tilde{Z}^{\mu\nu}, \end{aligned} \quad (38)$$

$$\mathcal{L}_{\eta_T W^+ W^-} = -\frac{g^2 N_{TC}}{48\pi^2 F_{\eta_T}} \left[N_2 - \frac{3}{2}N_1(N_{TC} - 1) \right] \eta_T W_{\mu\nu}^+ \tilde{W}^{-,\mu\nu}, \quad (39)$$

$$\mathcal{L}_{\pi_T^0 \gamma\gamma} = -\frac{e^2 N_{TC}}{8\pi^2 F_\pi} \left[Y_1 \cot \chi - \frac{3}{2}(N_{TC} - 1)Y_2 \tan \chi \right] \pi_T^0 F_{\mu\nu} \tilde{F}^{\mu\nu}, \quad (40)$$

$$\begin{aligned} \mathcal{L}_{\pi_T^0 Z\gamma} = & -\frac{e\sqrt{g^2 + g'^2} (1 - 4\sin^2 \theta_W) N_{TC}}{16\pi^2 F_\pi} \\ & \times \left[Y_1 \cot \chi - \frac{3}{2}(N_{TC} - 1)Y_2 \tan \chi \right] \pi_T^0 F_{\mu\nu} \tilde{Z}^{\mu\nu}, \end{aligned} \quad (41)$$

$$\begin{aligned} \mathcal{L}_{\pi_T^0 ZZ} = & \frac{(g^2 + g'^2) \sin^2 \theta_W (1 - 2\sin^2 \theta_W) N_{TC}}{16\pi^2 F_\pi} \\ & \times \left[Y_1 \cot \chi - \frac{3}{2}(N_{TC} - 1)Y_2 \tan \chi \right] \pi_T^0 Z_{\mu\nu} \tilde{Z}^{\mu\nu}. \end{aligned} \quad (42)$$

Recall that $N_1 = 1$ and $N_2 = 3(N_{TC} - 2)$ for the model in Eq. (1) and note that $1 + 4Y_i^2 = 2(Q_{Ui}^2 + Q_{Di}^2)$, twice the sum of the squares of technifermion T_i 's electric charges. Notice also the potential for cancellations between the T_1 and T_2 terms in these expressions that we mentioned above. This will have an especially striking effect on $\sigma B(gg \rightarrow \eta_T \rightarrow \gamma\gamma)$. A similar cancellation occurs between the $\eta_T \rightarrow \gamma\gamma$ and $\pi_T^0 \rightarrow \gamma\gamma$ amplitudes.

It is clear from these interactions that the rates for $\eta_{L,H} \rightarrow ZZ^* \rightarrow 4\ell$ and $\eta_{L,H} \rightarrow WW^* \rightarrow \ell\nu\ell\nu$ are very much less than $\eta_{L,H} \rightarrow \gamma\gamma$. The question of whether the ZZ^* and, to a lesser extent, the WW^* reported by ATLAS and CMS are real or poorly understood backgrounds should be resolved by the data expected this year. We will comment on $\eta_L \rightarrow Z\gamma$ rate in Sec. 5. Finally, with the complete mixing of Eq. (24), the coupling of $\eta_{L,H}$ to two electroweak bosons V_1 and V_2 is given by

$$\mathcal{L}_{\eta_{L,H}V_1V_2} = \sqrt{\frac{1}{2}} \left(\mathcal{L}_{\eta_T V_1V_2} \mp \text{sgn}(b_2) \mathcal{L}_{\pi_T^0 V_1V_2} \right). \quad (43)$$

Consider the $\eta_{L,H}\bar{f}f$ couplings now. From Eq. (26), they are determined by the ETC interactions coupling quarks and leptons to technifermions. These are the same interactions responsible for the SM fermions' masses (except for most of m_t) and it is therefore tempting to assume that the couplings to $\bar{f}f$ are simply of order m_f/F_{η_T} . This is naive, however. As discussed in Ref. [12, 44], a generic scenario for the fermions' ETC couplings in a two-scale model is that SM fermions f connect to T_1 and T_1 to T_2 . In walking technicolor, the one-loop f - T_1 - f graphs and the two-loop f - T_1 - T_2 - T_1 - f graphs can be comparable. Thus, it is not at all obvious that the sum of these two contributions to the η_T and π_T^0 couplings to $\bar{f}f$ have a simple proportionality to m_f . Therefore, we write

$$\begin{aligned} \mathcal{L}_{\eta_T \bar{f}f} &= i \sum_f \frac{\zeta_{\eta_T, f} m_f}{F_{\eta_T}} \eta_T \bar{f} \gamma_5 f, \\ \mathcal{L}_{\pi_T^0 \bar{f}f} &= i \sum_f \frac{\zeta_{\pi_T^0, f} m_f}{F_{\pi}} \pi_T^0 \bar{f} \gamma_5 f, \end{aligned} \quad (44)$$

where the factors ζ_f for η_T and π_T^0 will have to be fixed by experiment.⁷

5. $\eta_{L,H}$ Phenomenology

We begin with a comparison of the rates of gg fusion of $\eta_{L,H}$ and the SM Higgs. The coupling of H to two gluons is given to sufficient accuracy by

$$\mathcal{L}_{Hgg} = \frac{g_C^2}{48\pi^2 v} H G_{C,\mu\nu}^\alpha G_C^{\alpha,\mu\nu}. \quad (45)$$

Then, using $\mathcal{L}_{\eta_T gg}$ from Eq. (30), and assuming the complete mixing of Eq. (24) and $M_{\eta_{L,H}} = M_H$, we have

$$\frac{\sigma(gg \rightarrow \eta_{L,H})}{\sigma(gg \rightarrow H)} = \left(\frac{3N_1 N_{TC} (N_{TC} - 1)v}{4\sqrt{2}F_{\eta_T}} \right)^2 = \frac{9.8}{1 + 35 \sin^2 \chi}. \quad (46)$$

The second equality is for $N_{TC} = 4$, $N_1 = 1$ and $N_2 = 6$. If we use the limit $\sin \chi < 0.3$ obtained for LSTC with $M_{\rho_T} \lesssim 300 \text{ GeV}$ [37, 34], this ratio is $\gtrsim 2.5$. This production rate will be compensated by a small $B(\eta_L \rightarrow \gamma\gamma)$.

⁷Actually, there is no reason that these Yukawa interactions should be parity-conserving but, for our purpose here, this assumption is sufficient.

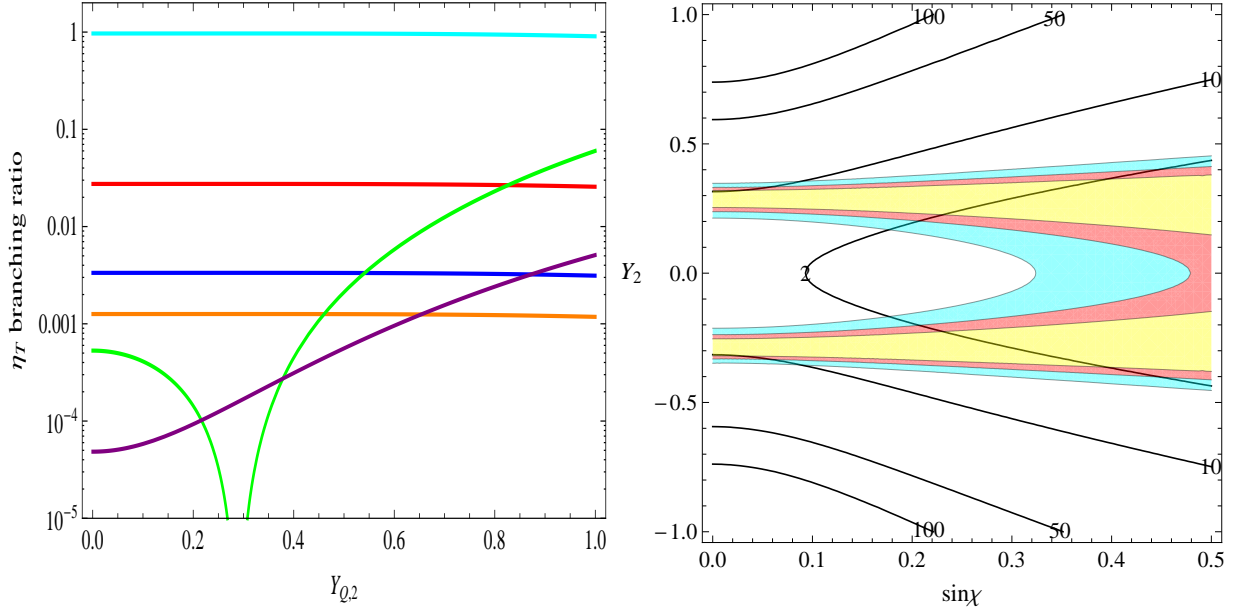


Figure 5: Left: The decay branching ratios as a function of Y_2 for a 125 GeV $\eta_T \rightarrow gg$ (teal), $\bar{b}b$ (red), $\tau^+\tau^-$ (blue), $\bar{c}c$ (orange), $\gamma\gamma$ (green) and $Z\gamma$ for a real photon and on-shell Z (purple). The WW^* and ZZ^* rates are negligible. See the text for how $\bar{f}f$ couplings are set. Right: The ratio $R_H = \sigma B(gg \rightarrow \eta_L \rightarrow \gamma\gamma) / \sigma B(gg \rightarrow H \rightarrow \gamma\gamma)$ for $M_{\eta_T} = M_H = 125$ GeV, as a function of $\sin\chi$ and Y_2 . $R_H < 1$ (yellow), $1.0 < R_H < 2.0$ (ochre), $2.0 < R_H < 4.0$ (teal). Overlaid on this plot are contours $\sigma B(gg \rightarrow \eta_T \rightarrow Z\gamma) / \sigma B(gg \rightarrow H \rightarrow Z\gamma)$.

In the rest of this section we present results assuming both zero η_T - π_T^0 mixing and complete mixing. They consist mainly of the $\eta_{L,H}$ decay branching ratios, the ratio $\sigma B(gg \rightarrow \eta_L \rightarrow \gamma\gamma) / \sigma B(gg \rightarrow H \rightarrow \gamma\gamma)$ for $M_H = M_{\eta_L} = 125$ GeV, and $\sigma B(gg \rightarrow \eta_H \rightarrow \gamma\gamma)$ versus the η_L -rate. The last assumes $M_{\eta_H} = 180$ GeV, a value corresponding to complete η_T - π_T^0 mixing at $M_{\pi_T^\pm} = 155$ GeV. We assume throughout that the T_1 hypercharge $Y_1 = 0$, which is strongly suggested by the absence of a signal for $\omega_T \rightarrow \ell^+\ell^-$ at the rate expected in LSTC for $M_{\omega_T} \simeq 300$ GeV [45]. The value $\sin\chi = 0.3$ is used to determine F_{η_T} and the π_T^0 couplings in the branching-ratio plots; it is varied for calculating the branching ratios in the σB plots. We assume ζ_τ and ζ_b factors that give the same σB as the SM Higgs.⁸

The η_T branching ratios and $\gamma\gamma$ rates are shown in Fig. 5 for the case of no mixing with π_T^0 . For $Y_1 = 0$, these are even functions of Y_2 . As anticipated, the zero in the $\gamma\gamma$ rate at $Y_2 = 0.29$ is due to a cancellation between the T_1 and T_2 contributions. For $\sin\chi < 0.3$, there are narrow bands ($\Delta Y_2 \simeq 0.07$) centered on $Y_2 = \pm 0.29$ where the $\eta_T \rightarrow \gamma\gamma$ rate is up to four times as large as the SM Higgs rate. We expect that any

⁸In more detail: For a specific η_T - π_T^0 mixing, we calculate ζ_f with $Y_1 = Y_2 = 0$. (There is only weak dependence on Y_2 .) Solving $\sigma B(\eta_L \rightarrow \bar{f}f) / (\sigma B(H \rightarrow \bar{f}f)) = 1$ for ζ_τ and ζ_b , and taking all ζ_f equal the larger of the two, gives ζ_f as a function of $\sin\chi$ for each η_T - π_T^0 mixing. The results presented here for gauge boson pair-production rates (mostly diphoton) are insensitive to ζ_f so long as $B(\eta_L \rightarrow \bar{f}f) \lesssim B(H \rightarrow \bar{f}f)$.

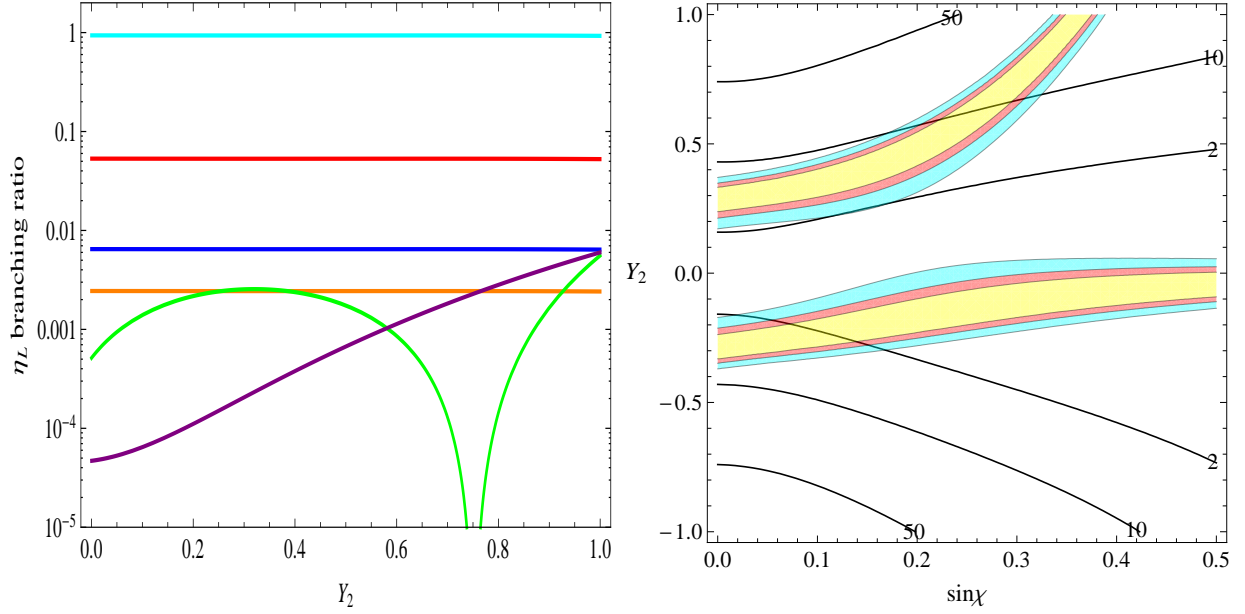


Figure 6: Left: The decay branching ratios as a function of Y_2 for a 125 GeV $\eta_L \rightarrow gg$ for the case of complete η_T - π_T^0 mixing with $\text{sgn}(b_2) > 0$. Right: The ratio $R_H = \sigma B(gg \rightarrow \eta_L \rightarrow \gamma\gamma) / \sigma B(gg \rightarrow H \rightarrow \gamma\gamma)$ for $M_H = M_{\eta_L} = 125$ GeV, as a function of $\sin \chi$ and Y_2 . Overlaid on this plot are contours $\sigma B(gg \rightarrow \eta_L \rightarrow Z\gamma) / \sigma B(gg \rightarrow H \rightarrow Z\gamma)$. The color codes are as in Fig. 5.

additional jets associated with this gg -production would be color-connected with the primary production and not exhibit a rapidity gap. Overlaid on this plot are contours giving the ratio $\sigma B(gg \rightarrow \eta_T \rightarrow Z\gamma) / \sigma B(gg \rightarrow H \rightarrow Z\gamma)$. The ratio is 2–10 for $\sin \chi < 0.3$. We have estimated the rate for $\eta_T \rightarrow Z\gamma^* \rightarrow 4\ell$ and found that, for a luminosity of 10 fb^{-1} , at most half an event would have been produced. After efficiencies, essentially none of the events in Fig. 2 could be due to this η_T decay.

The η_L branching ratios and $\gamma\gamma$ production rate compared to the SM Higgs are shown for the complete-mixing cases and $Y_1 = 0$ in Fig. 6 for $\text{sgn}(b_2) > 0$ and Fig. 7 for $\text{sgn}(b_2) < 0$. These two cases go into each other by reversing the signs of Y_1 and Y_2 . For $Y_1 = 0$ and $\sin \chi = 0.3$, the zero in $B(\eta_L \rightarrow \gamma\gamma)$ for $Y_2 > 0$ occurs for the two cases at 0.75 and 0.11, respectively. The allowed ranges of $\sigma B(\eta_L \rightarrow \gamma\gamma)$ occur in bands of thickness $\Delta Y_2 \simeq 0.2$ and, for the two mixing cases, they are mirror reflections of each other about $Y_2 = 0$ for $Y_1 = 0$. In these allowed regions, $B(\eta_L \rightarrow \gamma\gamma)$ is 4–10 times smaller than the SM Higgs branching ratio. As in the unmixed case, the $\eta_L \rightarrow Z\gamma$ rate is 2–10 times the SM Higgs rate, much too small to account for the data in Fig. 2.

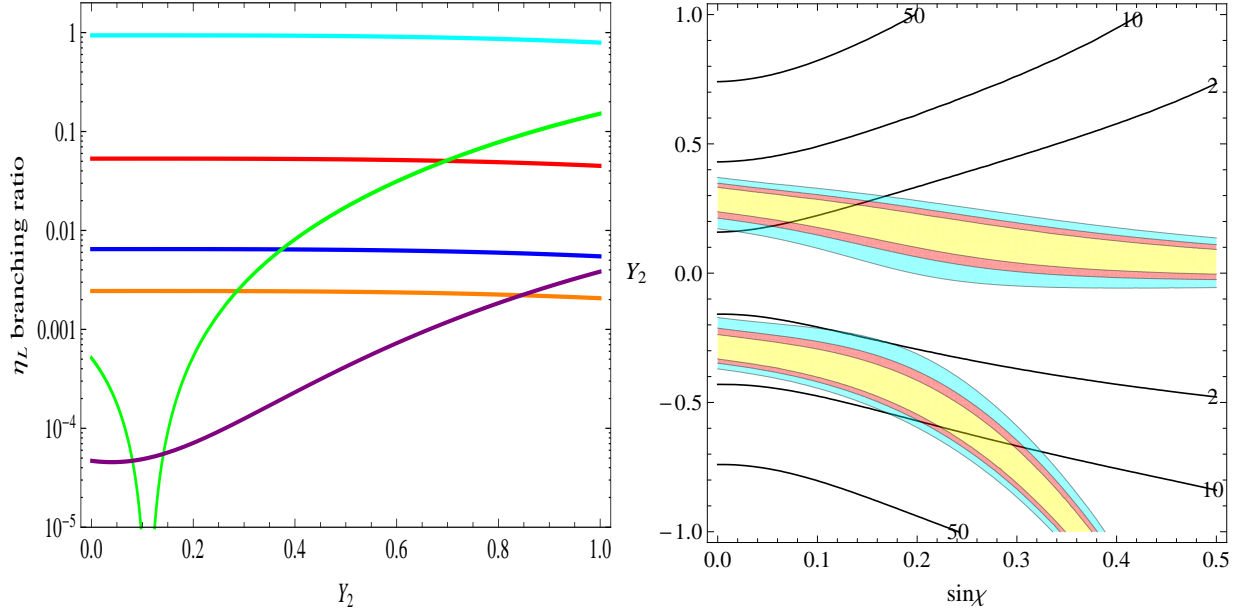


Figure 7: Left: The decay branching ratios as a function of Y_2 for a 125 GeV $\eta_L \rightarrow gg$ for the case of complete η_T - π_T^0 mixing with $\text{sgn}(b_2) < 0$. Right: The ratio $R_H = \sigma B(gg \rightarrow \eta_L \rightarrow \gamma\gamma) / \sigma B(gg \rightarrow H \rightarrow \gamma\gamma)$ for $M_H = M_{\eta_L} = 125$ GeV, as a function of $\sin \chi$ and Y_2 . Overlaid on this plot are contours $\sigma B(gg \rightarrow \eta_L \rightarrow Z\gamma) / \sigma B(gg \rightarrow H \rightarrow Z\gamma)$. The color codes are as in Fig. 5.

Finally, in Fig. 8 we overlay the $\sigma B(gg \rightarrow \eta_L \rightarrow \gamma\gamma) / \sigma B(gg \rightarrow H \rightarrow \gamma\gamma)$ ratios with contours of $\sigma B(gg \rightarrow \eta_H \rightarrow \gamma\gamma)$ given in picobarns. Based on a CMS search for diphoton resonances in 2.2 fb^{-1} of 7-TeV data [46], we estimate that $\sigma B(gg \rightarrow \eta_H \rightarrow \gamma\gamma) \lesssim 0.25 \text{ pb}$ is allowed. This is consistent with both branches of the green-shaded region of this figure for $|Y_2| < 0.4$.

6. η_T - π_T^0 Mixing and LSTC Collider Phenomenology

The discussion in this section is based on our interpretation of CDF's dijet excess as the production of a 280–290 GeV ρ_T which decays to a 150–160 GeV π_T plus a W -boson [30, 40, 33, 34].⁹ The π_T decays 90–95% of the time to $\bar{q}q$ jets (which may or may not contain b -jets, hence the spread we assume in M_{π_T} and M_{ρ_T}). With large η_T - π_T^0 mixing, however, the $\rho_T^\pm \rightarrow W\pi_T^0$ component of 150 GeV dijet signal is absent. This loss is replaced, to some extent, by $\rho_T \rightarrow W\eta_L \rightarrow \ell^\pm \nu jj$ with $M_{jj} \simeq 125$ GeV, with about half the dijets now being gg jets. Detailed calculation of this new phenomenology requires either a complete rewrite of the PYTHIA code for LSTC or a new implementation in another amplitude generator, and

⁹In Ref. [33] we found that $\simeq 25\%$ of the Tevatron signal was due to $a_T \rightarrow W\pi_T$, with $M_{a_T} = 1.1M_{\rho_T}$ assumed.

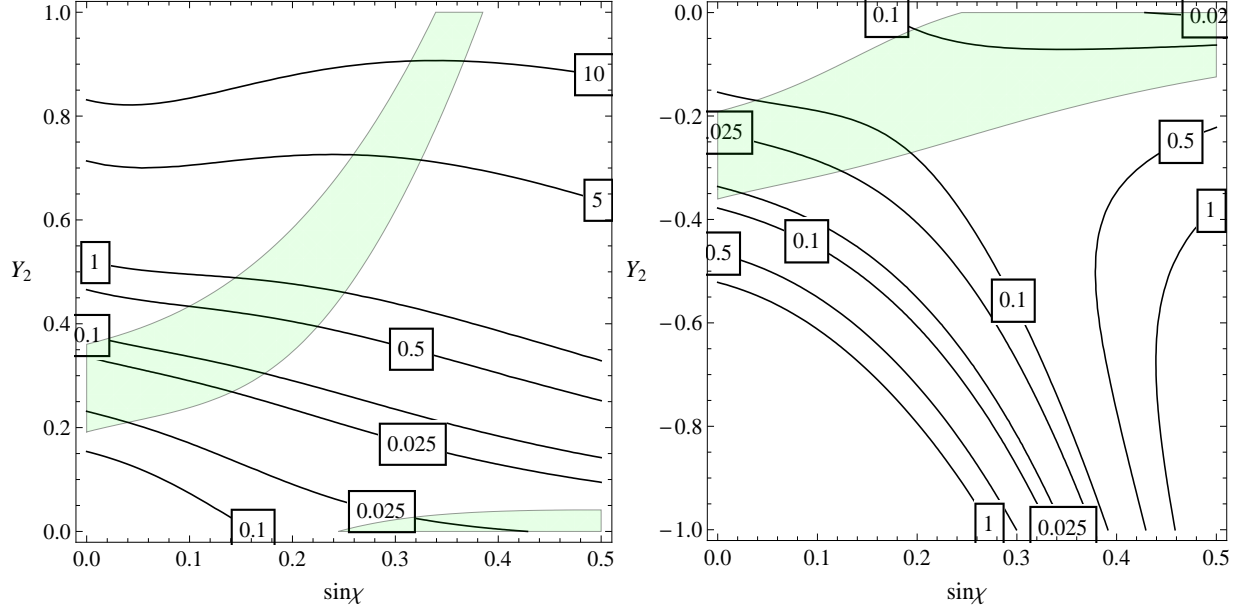


Figure 8: The green-shaded regions are $R_H = \sigma B(gg \rightarrow \eta_L \rightarrow \gamma\gamma) / \sigma B(gg \rightarrow H \rightarrow \gamma\gamma) < 4$ for $M_H = M_{\eta_L} = 125$ GeV and $\text{sgn}(b_2) > 0$, as a function of $\sin \chi$ and Y_2 . Overlaid on these plots are contours $\sigma B(gg \rightarrow \eta_H \rightarrow \gamma\gamma)$, in picobarns, for $M_{\eta_H} = 180$ GeV.

this is beyond the scope of our paper. Here we will be satisfied with a list of the important changes we anticipate.

- 1) The rate for $\rho_T, a_T \rightarrow W\pi_T$ is reduced. Simply (and naively) eliminating the $W\pi_T^0$ mode results in about a 35% reduction of the dijet excess signal [33].
- 2) There will be a $\rho_T, a_T \rightarrow W\eta_L \rightarrow \ell\nu jj$ signal at $M_{jj} \simeq 125$ GeV, largely due to its $W\pi_T^0$ component. The dijet peak may overlap somewhat with the $\rho_T^0 \rightarrow W^\pm \pi_T^\mp$ dijet excess. While $\rho_T, a_T \rightarrow W\eta_L$ is suppressed by the mixing, it is enhanced by the greater phase space and, so, may not be much smaller than the $W^\pm \pi_T^\mp$ rate. Note that this will appear as associated production of η_L with W , but the Wjj invariant mass will peak near M_{ρ_T} . There is *no* significant associated production of η_L with Z .
- 3) The channel $\rho_T^\pm \rightarrow \pi_T^\pm \eta_L$ is open and the π_T^0 component of this amplitude is a strong process, unsuppressed by $\sin \chi$. Even though the Q -value for this decay is only ~ 5 GeV, this mode could be an important part of the ρ_T^\pm width and its production rate might be as large ~ 500 fb at the LHC. We do not know of any limit on this four-jet process, especially since the two dijets have rather different masses.
- 4) A primary confirmation signal at the LHC for the CDF dijet excess is $\rho_T^\pm \rightarrow Z\pi_T^\pm \rightarrow \ell^+ \ell^- jj$. In Ref. [34], we predicted a rate of 190 fb for this final state (220 fb for $Y_1 = 0$ and $\sin \chi = 0.3$). This rate is likely diluted by the open $\pi_T^\pm \eta_L$ channel; a *rough* estimate

is a 50–60% reduction. This is an unfortunate hit to an otherwise very promising channel for this year’s data.

- 5) A similar reduction in the rate for $\rho_T^\pm \rightarrow WZ \rightarrow 3\ell\nu$ or $\ell^+\ell^-jj$ is to be expected. This eliminates the bound $\sin\chi < 0.3$ implied by the recent CMS data [37]. On the other hand, the idea of low-scale TC does not make much sense if $\sin\chi \gtrsim \frac{1}{2}$.
- 6) Last, though not least, we again urge a search for $\eta_H \rightarrow \gamma\gamma$ near 180 GeV. Over most of the allowed regions in Fig. 8, $\sigma B(\eta_H \rightarrow \gamma\gamma) \lesssim 0.25$ pb at the LHC. The upper end of this range should be accessible soon—if not already excluded.

7. Conclusions

The “Higgs impostor” proposal made in this paper is motivated both by our desire for a technicolor explanation for the new boson $X(125)$ and by the discrepancies in the current data with a standard-model Higgs explanation. To us, the most important discrepancy is the CMS ZZ^* data—the low number of real Z ’s—and its disagreement with the ATLAS ZZ^* data. This may just be statistics at work and be resolved in favor of the popular Higgs description when the next large batch of data is released. But, as we said at the outset, the SM Higgs outcome would confront theorists anew with the long-standing thorny questions of naturalness, hierarchy and flavor. If, on the other hand, the discrepancies in the data are real, then we may, at long last, have begun to unravel the mystery of electroweak symmetry breaking. That is a lot to hope for.

In this paper we proposed an alternative to the SM Higgs interpretation: $X(125)$ is a technipion, η_L . Our proposal has several immediately testable consequences in addition to discrediting the $X \rightarrow ZZ^*, WW^*$ data. Chief among these is that there is likely to be another Higgs impostor state η_H not far from 200 GeV, which may be visible in the diphoton spectrum. If the CDF dijet excess is real, and our LSTC interpretation of it correct, then $M_{\eta_H} = 170\text{--}190$ GeV. Furthermore, the M_{jj} spectrum in the range 170–200 GeV range is contaminated by a sizable $\rho_T \rightarrow W\eta_L$ component that will complicate modeling in terms of standard diboson production [47].

Acknowledgments

We are grateful to T. Appelquist, W. Bardeen, K. Black, T. Bose, P. Catastini, A. DeRoeck, C. Fantasia, C. Hill, K. Terashi, B. Zhou and J. Zhu for valuable conversations and advice. This work was supported by Fermilab operated by Fermi Research Alliance, LLC, U.S. Department of Energy Contract DE-AC02-07CH11359 (EE and AM) and in part by the U.S. Department of Energy under Grant DE-FG02-91ER40676 (KL). KL’s research was also supported in part by Laboratoire d’Annecy-le-Vieux de Physique Theorique (LAPTh) and the CERN Theory Group and he thanks LAPTh and CERN for their hospitality.

References

- [1] **ATLAS Collaboration** Collaboration, G. Aad *et. al.*, “Observation of a new particle in the search for the Standard Model Higgs boson with the ATLAS detector at the LHC,” *Phys.Lett.* **B716** (2012) 1–29, 1207.7214.
- [2] **CMS Collaboration** Collaboration, S. Chatrchyan *et. al.*, “Observation of a new boson at a mass of 125 GeV with the CMS experiment at the LHC,” *Phys.Lett.* **B716** (2012) 30–61, 1207.7235.
- [3] S. Glashow, “Partial Symmetries of Weak Interactions,” *Nucl.Phys.* **22** (1961) 579–588.
- [4] S. Weinberg, “A Model of Leptons,” *Phys.Rev.Lett.* **19** (1967) 1264–1266.
- [5] A. Salam, “Weak and Electromagnetic Interactions,” *Conf.Proc.* **C680519** (1968) 367–377.
- [6] F. Englert and R. Brout, “Broken Symmetry and the Mass of Gauge Vector Mesons,” *Phys.Rev.Lett.* **13** (1964) 321–323.
- [7] P. W. Higgs, “Broken symmetries, massless particles and gauge fields,” *Phys.Lett.* **12** (1964) 132–133.
- [8] G. Guralnik, C. Hagen, and T. Kibble, “Global Conservation Laws and Massless Particles,” *Phys.Rev.Lett.* **13** (1964) 585–587.
- [9] L. Susskind, “Dynamics of Spontaneous Symmetry Breaking in the Weinberg-Salam Theory,” *Phys.Rev.* **D20** (1979) 2619–2625.
- [10] G. ’t Hooft, “Naturalness, chiral symmetry, and spontaneous chiral symmetry breaking,” *NATO Adv.Study Inst.Ser.B Phys.* **59** (1980) 135.
- [11] S. Weinberg, “Implications of Dynamical Symmetry Breaking: An Addendum,” *Phys.Rev.* **D19** (1979) 1277–1280.
- [12] K. D. Lane and E. Eichten, “Two Scale Technicolor,” *Phys. Lett.* **B222** (1989) 274.
- [13] K. Lane and A. Martin, “An Effective Lagrangian for Low-Scale Technicolor,” *Phys. Rev.* **D80** (2009) 115001, 0907.3737.
- [14] A. Delgado, K. Lane, and A. Martin, “A Light Scalar in Low-Scale Technicolor,” *Phys.Lett.* **B696** (2011) 482–486, 1011.0745.
- [15] S. Matsuzaki and K. Yamawaki, “Techni-dilaton at 125 GeV,” *Phys.Rev.* **D85** (2012) 095020, 1201.4722.

- [16] S. Matsuzaki and K. Yamawaki, “Discovering 125 GeV techni-dilaton at LHC,” 1206.6703.
- [17] D. D. Dietrich, F. Sannino, and K. Tuominen, “Light composite Higgs from higher representations versus electroweak precision measurements: Predictions for LHC,” *Phys. Rev.* **D72** (2005) 055001, hep-ph/0505059.
- [18] D. Elander and M. Piai, “The decay constant of the holographic techni-dilaton and the 125 GeV boson,” 1208.0546.
- [19] Z. Chacko, R. Franceschini, and R. K. Mishra, “Resonance at 125 GeV: Higgs or Dilaton/Radion?,” 1209.3259.
- [20] B. Bellazzini, C. Csaki, J. Hubisz, J. Serra, and J. Terning, “A Higgslike Dilaton,” 1209.3299.
- [21] W. D. Goldberger, B. Grinstein, and W. Skiba, “Distinguishing the Higgs boson from the dilaton at the Large Hadron Collider,” *Phys.Rev.Lett.* **100** (2008) 111802, 0708.1463.
- [22] I. Low, J. Lykken, and G. Shaughnessy, “Singlet scalars as Higgs imposters at the Large Hadron Collider,” *Phys.Rev.* **D84** (2011) 035027, 1105.4587.
- [23] I. Low, J. Lykken, and G. Shaughnessy, “Have We Observed the Higgs (Imposter)?,” 1207.1093.
- [24] R. S. Chivukula, B. Coleppa, P. Ittisamai, H. E. Logan, A. Martin, *et. al.*, “Discovering Strong Top Dynamics at the LHC,” 1207.0450.
- [25] B. Coleppa, K. Kumar, and H. E. Logan, “Can the 126 GeV boson be a pseudoscalar?,” 1208.2692.
- [26] M. T. Frandsen and F. Sannino, “Discovering a Light Scalar or Pseudoscalar at The Large Hadron Collider,” 1203.3988.
- [27] **The CMS Collaboration** Collaboration, J. Incandela, “Status of the CMS SM Higgs Search, July 4, 2012,”.
- [28] **CDF Collaboration, D0 Collaboration** Collaboration, T. Aaltonen *et. al.*, “Evidence for a particle produced in association with weak bosons and decaying to a bottom-antibottom quark pair in Higgs boson searches at the Tevatron,” 1207.6436.
- [29] **CDF Collaboration** Collaboration, T. Aaltonen *et. al.*, “Search for the standard model Higgs boson decaying to a $b\bar{b}$ pair in events with no charged leptons and large missing transverse energy using the full CDF data set,” *Phys.Rev.Lett.* **109** (2012) 111805, 1207.1711.

- [30] **CDF Collaboration**, T. Aaltonen *et. al.*, “Invariant Mass Distribution of Jet Pairs Produced in Association with a W boson in ppbar Collisions at $\sqrt{s} = 1.96$ TeV,” *Phys. Rev. Lett.* **106** (2011) 171801, 1104.0699.
- [31] J. Wess and B. Zumino, “Consequences of anomalous Ward identities,” *Phys. Lett.* **B37** (1971) 95.
- [32] E. Witten, “Global Aspects of Current Algebra,” *Nucl. Phys.* **B223** (1983) 422–432.
- [33] E. J. Eichten, K. Lane, and A. Martin, “Technicolor Explanation for the CDF W_{jj} Excess,” *Phys.Rev.Lett.* **106** (2011) 251803, 1104.0976.
- [34] E. Eichten, K. Lane, A. Martin, and E. Pilon, “Testing the Technicolor Interpretation of the CDF Dijet Excess at the 8-TeV LHC,” 1206.0186.
- [35] A. G. Cohen and H. Georgi, “WALKING BEYOND THE RAINBOW,” *Nucl. Phys.* **B314** (1989) 7.
- [36] C. T. Hill, “Topcolor assisted technicolor,” *Phys. Lett.* **B345** (1995) 483–489, hep-ph/9411426.
- [37] **CMS Collaboration** Collaboration, S. Chatrchyan *et. al.*, “Search for exotic particles decaying to WZ in pp collisions at $\sqrt{s}=7$ TeV,” 1206.0433.
- [38] E. Eichten and K. D. Lane, “Dynamical Breaking of Weak Interaction Symmetries,” *Phys. Lett.* **B90** (1980) 125–130.
- [39] K. Lane and S. Mrenna, “The collider phenomenology of technihadrons in the technicolor Straw Man Model,” *Phys. Rev.* **D67** (2003) 115011, hep-ph/0210299.
- [40] **CDF Collaboration** <http://www-cdf.fnal.gov/physics/ewk/2011/wjj/7-3.html>.
- [41] R. F. Dashen, “Chiral $SU(3) \times SU(3)$ as a symmetry of the strong interactions,” *Phys. Rev.* **183** (1969) 1245–1260.
- [42] T. Sjostrand, S. Mrenna, and P. Z. Skands, “PYTHIA 6.4 Physics and Manual,” *JHEP* **0605** (2006) 026, hep-ph/0603175.
- [43] J. A. Harvey, C. T. Hill, and R. J. Hill, “Standard Model Gauging of the Wess-Zumino-Witten Term: Anomalies, Global Currents and pseudo-Chern-Simons Interactions,” *Phys. Rev.* **D77** (2008) 085017, 0712.1230.
- [44] K. D. Lane and M. V. Ramana, “Walking technicolor signatures at hadron colliders,” *Phys. Rev.* **D44** (1991) 2678–2700.

- [45] **ATLAS Collaboration** Collaboration, G. Aad *et. al.*, “Search for high-mass resonances decaying to dilepton final states in pp collisions at a center-of-mass energy of 7 TeV with the ATLAS detector,” 1209.2535.
- [46] **CMS Collaboration** Collaboration, S. Chatrchyan *et. al.*, “Search for signatures of extra dimensions in the diphoton mass spectrum at the Large Hadron Collider,” 1112.0688.
- [47] **CMS Collaboration** Collaboration, S. Chatrchyan *et. al.*, “Study of the dijet mass spectrum in $pp \rightarrow W + \text{jets}$ events at $\sqrt{s} = 7$ TeV,” 1208.3477.